January 1992

A Spatially Distributed Water Balance Based on Physical, Isotropic and Airborne Remotely Sensed Data

C. M.U. Neale

David G. Tarboton

J. J. McDonnell

A Spatially Distributed Water Balance Based on Physical, Isotropic and Airborne Remotely Sensed Data

Annual Technical Report submitted to the
U.S. Geological Survey

Award No. 14-08-0001-G2110

C.M.U. Neale
D.G. Tarboton
J.J. McDonnell

Utah State University
Utah Water Research Laboratory
Logan, UT 84322-8200
(801) 750-3172

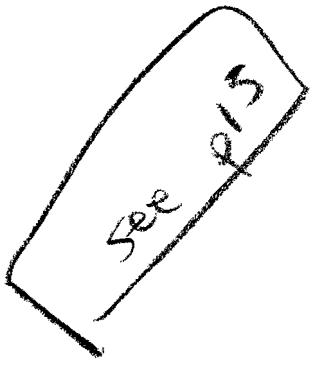

November 1992

Table of Contents

Table of Contents (Cont'd)

List of Tables

List of Figures

Introduction

The objective of this research to develop a spatially distributed water balance model based on the integration of spatially distributed data. Progress this year has consisted of model development, instrument acquisition, installation and development of experimental procedures, and baseline data collection.

The original research plan called for detailed observations related to the water balance over the year September 1991 to August 1992. The detailed measurements were to start with accumulation of the snowpack followed by melt and evapotranspiration measurements from March to August. The objective was to measure the energy balance parameters starting with the peak accumulation, through the melt and infiltration phases, the greenup of vegetation, the peak evapotranspiration period and the dry-down and senescence of grasses and other species in the Upper Sheep Creek sub-basin of the Reynolds Creek Experimental Watershed. Groundwater depths as well as run-off in the stream were to be measured and samples of the snowpack water, soil water, groundwater and run-off water were to be taken for isotopic tracing.

Unfortunately, average snow accumulation was well below average last winter. April 1st, snow course measurements indicated that the snowpack at the Reynolds mountain sub-basin was only 30% of normal. In the Upper Sheep Creek sub-basin, which usually has a 10-m high drift during this time of the year there was less than 0.5 m of snow. After consultation with the USDA scientists from the Northwest Watershed Research Center, we decided in February to postpone the field campaign for one year. In retrospect this was wise because there was no runoff response from Upper Sheep Creek (the basin where we plan to do our detailed model development) and few of the groundwater wells had measurable response, we would have had nothing to measure.

The intensive field campaign will be conducted in Spring 1993. Although a repeat of last year's condition is possible, the chances are very low and we are hopeful of better snowfall. A revised project time schedule is shown on the next page. This has us finishing the field measurements in August 1993. Given this it is unlikely that all data reduction and modeling will be complete by August 15, 1993 so we will need until May 1993, a 9-month no-cost extension to complete the data analysis.

In this report we describe our progress in terms of data base development, model development, and modeling based on data from earlier years. Some of this will be presented at the AGU Fall meeting in San Francisco in December (see abstract on page 3). We also developed snow-isotope fractionation studies, evapotranspiration model development, installation of soil moisture measurement equipment, and database development.

Revised Project Time Schedule

AGU Presentation Abstract

(EOS, Transactions, American Geophysical Union, 73(43), 1992, p. 243).

H52E-13 1655h

An Areally Distributed Hydrologic Model for an Arid Mountain Watershed

T.H. Jackson. (Utah Water Research Laboratory, Utah State University, Logan, Utah 84322-8200; ph 801-750-3151); D G Tarboton (Utah Water Research Laboratory, Utah State University, Logan, Utah 84322-8200; ph 801-750-3151); K R Cooley (USDA-ARS, Northwest Watershed Research Center, Boise, ID; ph 208-334-1363).

A distributed mass balance approach is being developed to model spatially variable hydrologic processes in an arid mountain watershed. The model will be applied to Upper Sheep Creek, a 26 ha catchment within the Reynolds Creek ARS Experimental Watershed, near Boise, ID.

The model is based on a DEM representation of basin topography. A mass balance equation relating moisture inflow, outflow, and the change in storage is resolved to give the moisture defecit in each DEM cell. Moisture input is subsurface flow from up-gradient DEM cells and surface infux from rain or a spatially distributed energy-balance snowmelt model. Subsurface outflow is determined from topographic slope and transmissivity, which is a function of moisture content.

We illustrate the effects of topography on the areal distribution of soil moisture and the time variation of streamflow in Upper Sheep Creek and compare our results with field observations and streamflow measurements.

Data Gathering and Processing

Topography and Digital Evaluation Model

The six USGS digital elevation model (DEM) quadrangles that cover Reynolds Creek Experimental Watershed have been acquired and processed. Upper Sheep Creek has been the focus of our model development work. Upper Sheep Creek is a steep 26-hectare "zero-order" watershed with an outlet elevation of about 1840 m, rising along a 975-m long main channel to an elevation of 2040 m. Figure 1 shows Upper Sheep Creek as mapped from the USGS DEM. When this is compared to contours from a detailed map prepared by the Aerial Mapping Company of Boise (Figure 2), one sees that the USGS DEM suffers from considerable smoothing and distortion. We have, therefore, developed a local DEM by digitizing information from the detailed map for use in high resolution modeling. This DEM has been constructed to coincide with the 30.48 x 30.48m (100 ft) grid used by the ARS to reference instrument location and as a horizontal control for the survey of snow water equivalent and depths . Figure 3 shows Upper Sheep Creek mapped in this DEM. Development of this DEM has resolved problems of inaccurate topography within Upper Sheep Creek. However, high resolution data is not available for other parts of Reynolds Creek experimental watershed, so the USGS DEM will have to be used. Our study will be able to determine its impact on model results.

Site Soil Data

A parameterization of the variation of saturated hydraulic conductivity with depth is a key element in the distributed hydrologic model being developed for Upper Sheep Creek. The present parameterization requires an estimate of surface saturated conductivity (k_S) and an exponential "decay coefficient" (f) describing how quickly the permeable layer is "pinched off." Estimating these parameters is facilitated by consulting soil maps.

A soil-type matrix site for the site was prepared by locating the ARS grid on soil maps of the Reynolds Creek Watershed [Stephenson, 1977]. The location of the five soil types identified within the Upper Sheep Creek catchment are shown in Figure 4, which shows the soil type assigned to each node of the ARS grid. The five soil categories are:

1. GaG; Gabica cobbly gravelly loam, 30-60% slopes
2. HmG; Harmehl & Demast stony loams, 30-60% slopes
3. GfF; Gabica very stony loam, 0-30% slopes
4. HbF; Harmehl gravelly loam, 0-30% slopes
5. GfG; Gabica very stony loam, 30-60% slopes

Stephenson [1977] does not give an estimate of soil permeability as is common in the USDA county soil map series. The closest coverage of USDA soil maps was in the publication "Elmore County Area, Idaho, Parts of Elmore, Owyhee, and Ada Counties." Of the five soils identified on site, only the Demast series is described in this publication. The permeability of this soil is listed as between 0 and 15 mm/hour.

Figure 1

Figure 2

Figure 3

Figure 4

Mock [1988] measured surface field saturated conductivity using a Guelph permeameter at over 60 points in the southwest corner of the site--including some measurements in Demast soils. He reports a range of permeability between 0.25 and 1.58 mm/hour, confirming the order of magnitude of these values. But without field measurements in other parts of the catchment and in the absence of information on the permeabilities of all the soil series on site, the use of an average permeability across the site seems adequate at present.

The descriptions of the soil horizons in each soil and geophysical measurements taken at the site will be used as aids in estimating distributed values of "f" at a later date.

ARS Snow Surveys

Distributed measurements of snow water equivalent at Upper Sheep Creek are available for six days in 1986 as summarized in Table 1:

Table 1. Summary of ARS snow surveys at Upper Sheep Creek[1], 1986

Survey Date:		Cells w/Snow:		Snow Volume[2] [m^3 of water equivalent]		
Julian	Common	New	Total	New	On Ground	Total
56	2/25	108	108	45951	45951	45951
85	3/26	13	85	2690	38315	48641
100	4/10	1	38	233	25975	48874
133	5/13	4	23	698	15128	49573
147	5/27	0	12	0	5835	49573
154	6/3	0	3	0	969	49573

[1]Based on the ARS grid, there are 255 node-centered cells in the watershed measuring 30.48 meters on each side.

[2]Snow volumes are calculated assuming the snow water equivalent depth reported at the grid point is distributed uniformly over the area of the cell.

The areal extent of the snow drift during each of the six surveys reported for the 1986 spring melt season is shown in Figure 5. Snow drifts are located on the north facing slope of the watershed. The "footprints" of the two main drifts on day 56 coincide with the Gabica soil types GfF and GfG (Zones 3 and 5 in Figure 4). Contours of snow water equivalent during the first four surveys are shown in relation to the main stream channel in Figure 6.

The data from these surveys were placed in six files for use as input in simulations as described below.

Figure 5

Figure 6

Site Weather Data

ARS weather data presently available for Upper Sheep Creek for the winter of 1985-6 includes the following:

1. Average Air Temperature, degrees Centigrade
2. Wind Run and Direction, miles & degrees respectively
3. Solar Radiation, Langleys/hour
4. Accumulated and Instantaneous Precipitation, inches.

ARS files for 1985 and 1986 have been processed and "spliced" together for use as input in the hydrologic simulations described below.

Water Balance Model

Considerable progress has been made in the development of distributed water balance "shell" for use in hydrologic modeling. This is a computational framework for the calculation of a water balance at each grid cell over a distributed watershed. Flow directions (surface and subsurface) are determined from digital elevation data (digitized topography) and flow rates are a function of slope, moisture content and soil parameters. One feature of our approach is that it allows outflow from a grid cell to be assigned fractionally to down slope cells, thus avoiding the problem of grid direction bias present in earlier work with digital elevation data. The water balance shell incorporates the effect of topography into hydrologic modeling. Topography controls the convergence and divergence of flow, crucial in the determination of moisture availability. Our modeling shell is designed to interact with other hydrologic process models, such as snowmelt and evapotranspiration, to provide a complete distributed water balance.

In the continuing development, versions of the model have been written to utilize surface inputs represented in different forms as discussed below.

All models can be divided into the four basic sections listed below, as discussed in the following subsections.

1. Input data and set run parameters
2. Calculate initial conditions and basin deficit
3. Hydrologic simulation, for each time step:
   a. Get surface influx to each cell
   b. Calculate mass balance recursively
   c. Update basin deficit and check basin-wide mass balance for basin during time step
4. Check basin-wide mass balance over total time of simulation

Input Data Run Parameters

"Run parameters" include the time step, the total number of timesteps to simulate, and other values used as flags in the control of program flow and to direct output to appropriate files.

Soil data that are input for each cell and remain constant over the simulation include porosity, surface saturated hydraulic conductivity, and a parameter, f, used to describe the variation of saturated permeability with depth. Input is in the form of matrices with the data records input in the order that they would appear on a map read from left to right, top to bottom. A header record gives the number of rows and columns and the horizontal and vertical spacing of the data.

Using the soil information discussed above, the values are set for each cell. It is difficult to evaluate the accuracy of the values assigned to each parameter. This is one of the key areas of work to be done.

A value of surface flux must be input for each cell during each time step. The simplest model uses an input hyetograph of rainfall, assumed to be uniformly distributed in the watershed. This formulation is most useful in the evaluation of the soil parameters assigned to each cell. The second model uses a spatially variable surface influx estimated from the changes in the depth of snow at each cell during the six ARS snow surveys described above. These point fluxes remain constant between the survey dates.

A snow melt model is presently being refined to link with the mass balance model. This will give a surface flux with a spatial and temporal variation. The snowmelt model is an energy balance requiring measurements of temperature, wind speed, relative humidity and precipitation. Time traces for all of these measurements are presently available, except for relative humidity; it is provisionally calculated for each hour assuming that the daily minimum temperature is the dew-point for that day.

Long- and short-wave radiation fluxes are calculated from "almanac functions" dependent on calendar date and longitude and cell-dependent functions that are calculated by the mass balance shell: slope, aspect, and elevation. The calculated total incident radiation will be compared with the measured radiation.

Initial Conditions and Basin Deficit

The basic mass balance equation for constant density, unsteady flow, written in terms of deficits rather than storage is

$$\frac{dD}{dt} = \frac{d}{dt}(z.n.dx.dy) = O(t) - I(t) \qquad (1)$$

where z is the depth to the water table, ignoring unsaturated flow. This value, z, is a state variable for each cell.

The initial deficit of water in the basin is determined by assigning an initial groundwater outflow from each cell equal to a fraction of the initial, measured flow over the main channel outlet weir, assuming that there is no leakage from the basin. The fraction is taken as the upstream contributing area for each cell divided by the total basin area. The groundwater outflow equation is then solved at each cell to give its initial deficit. If the maximum groundwater that can be conveyed from a cell is less than the value assigned by its fraction of basin area, it is assumed to be saturated (zero deficit).

This method preserves mass balance, of course, by definition. It can be used as a check on the assignment of soil parameters by comparing the initial deficits with soundings from piezometers, if they are available for the starting day of the simulation.

Hydrologic Simulation

The flux terms in the deficit balance equation are inflow and outflow. Inflow consists of surface influx, where present, and groundwater flow from upstream cells,where present. Outflow is determined by the product of transmissivity and surface slope of each cell. When outflow exceeds the cell's conveyance, the cell is saturated and excess water becomes surface runoff.

Surface slope is determined for each cell in the direction of the eight surrounding cells. Flow is apportioned in all directions with a positive gradient in proportion to the weighted slope. If each cell's hydraulic conductivity declines with an exponential factor f with increasing depth z, measured positive downwards, groundwater outflow from each cell can be obtained from integration as:

$$O(t) = \frac{k_s dy}{f} \sum_{k=1}^{8} \max [0, Sg_k w_k] e^{-fz} \qquad (2)$$

where dy is the width of the cell, Sg_k is the local ground slope in direction k (positive downward) and w_k is a factor to account for the width of flow in each direction. Taking the maximum of 0 and $Sg_k w_k$ serves to only sum over those directions with positive downslope direction. The deficit balance equation can be written as:

$$\frac{dz}{dt} = \frac{k_s \cdot \sum_{k=1}^{8} \max [0, Sg_k w_k]}{f.n.dx} e^{-fz} - \frac{I(t)}{n.dx.dy} \qquad (3)$$

where

$$I(t) = \sum (\text{gw inflow neighbors}) + \text{Surface Influx} \qquad (4)$$

For a given time step, all values in the equation are known at the time of solution except for the deficit z, so equation (3) may be written as:

$$\frac{dz}{dt} = C_1 e^{-fz(t)} - C_2 \qquad (5)$$

where C_1 and C_2 are constants. What is termed as the "hydrologic simulation" is a solution of this mass balance equation for each cell at each step. This is done by a call from the main program to a mass balance function that calls itself recursively to solve the deficit balance equation "in the downstream direction," that is, the equations are solved first for "ridge line" cells with no upslope inflows. The deficit balance equation is solved for the deficit, giving z and the outflow, which becomes the inflow to cells down gradient. Runoff in excess of conveyance capacity is routed downstream without being allowed to reinfiltrate.

The basin wide mass balance at each step is checked by summing the surface influx to each cell and the outflow from the basin. The total basin deficit is calculated by summing the deficit of each cell. The difference between the change in deficit and the net basin outflow (weir discharge plus

evaporation losses less precipitation) is a check that the equations are coded correctly and a measure of the numerical accuracy of the equations because mass balance closure is implicit in the formulation. The ability of the model to represent hydrologic processes can only be verified by measuring fluxes at points in the field.

Model Runs to Date

A simple version of the model was developed first to check program logic. In this first model, surface influx was in the form of precipitation distributed uniformly over the watershed. Soil parameters were taken as constant across the watershed.

The next level of refinement was to incorporate the spatial variation of surface influx to the model in the form of snowmelt. The ARS Snow surveys, described above, were used as the basis for estimating surface the influx to each cell. The change in the depth of snow water equivalent between each pair of survey dates was taken as the constant rate of snowmelt percolating into the soil for each cell during that period. This ignores evaporation and sublimation, so basin runoff is overestimated in the later part of the season.

Runs of the model with this input have shown that the model is stable with respect to the time step used. Figure 7 shows a comparison of simulated and observed hydrographs for the watershed during the 1985-86 season. The model correctly simulates the times and the gross magnitude of the peak discharges and the total seasonal volume of runoff but does not accurately reflect the instantaneous flow rate outside of peak times. This is partly due to the crude estimate of the rate of snowmelt used as input.

The distributed mass balance shell is presently being modified to accept surface influxes as determined by an energy balance-based calculation of snowmelt applied at each DEM cell at each time step.

The mass balance equation will be modified to include unsaturated zone storage. A kinematic wave approximation will be used to simulate the infiltration of rainwater and snowmelt from the ground surface to the water table.

An evaporation model will be used to model soil water depletion during the dry season.

Snowmelt Model

We have developed a snowmelt model that is based on a physical parameterization of all energy exchanges and yet retains a simple lumped nature, requiring only two state variables (energy content and water equivalent) to characterize the snowpack. Testing of this model is still ongoing. In this report we provide a detailed description of this model and results from tests done to date.

State Variables

In the model, snowpack is characterized by two state variables, water equivalent, W[m], and energy content U, [kJ/m^2]. These variables are, we believe, sufficient to characterize the snowpack for the prediction of melt rates that cause erosion. Other time-varying snowpack properties such as density and albedo play a secondary role. Future work will investigate the importance of these, as well as variations within the snowpack in terms of a one-dimensional or multi-layer model. The state variable, energy content U, is defined relative to a reference state of water at 0°C in the ice (solid) phase. U greater than 0 means the snowpack (if any) is isothermal with some liquid content and U less than 0 can be used to calculate the snowpack average temperature, T, [°C]. Energy content is defined as the energy content of the snowpack plus a top

Figure 7

layer of soil with depth D_e [m]. This provides a simple buffering against numerical instabilities when the snowpack is shallow, as well as simple approximations of frozen ground and melting of snow falling on warm ground. We discuss below the choice of D_e and the role it plays in the model.

Driving Variables

Our model is designed to be driven by the following inputs at each time step.

- Air Temperature, Ta, [°C]

- Wind Speed, V, [m/s]

- Relative Humidity, RH

- Precipitation, P, [m/hr]

- Cloud Cover Fraction, N

- Ground Heat Flux, Q_g, [kJ/m^2/hr], [assumed a small amount of 50 in all results below]

Cloud fraction N is used to calculate incoming solar and long-wave radiation. In the event that N is not available, we use an empirical approximation due to Leavesley et al. [1983], based on daily maximum air temperature to modulate incoming radiation.

Site and Initial Variables

The variables required to characterize the site are:

- Slope - θ (degrees)

- Aspect - Az (degrees, clockwise from north of the steepest downslope vector)

- Latitude (degrees)

- Elevation (m)

In future work we plan to incorporate the effect of vegetation and site variables such as leaf area index or cover density will be required. The model needs to be given initial values of the state variables U and W, as well as, the start date and time step.

Parameters

Model parameters and their recommended value are listed in Table 2. Most of these are known constants. Those that are adjustable are shown. Some of these could also be interpreted as site variables.

Table 2. Snowmelt Model Parameters

I_o	Solar Constant	4914	kJ m^{-2} h^{-1}	
C_s	Ice Heat Capacity	2.09	kJ kg^{-1} $°C^{-1}$	
C_w	Water Heat Capacity	4.18	kJ kg^{-1} $°C^{-1}$	
C_g	Ground Heat Capacity	2.1	kJ kg^{-1} $°C^{-1}$	Adjustable
C_p	Air Heat Capacity at Constant Pressure	1.005	kJ kg^{-1} $°C^{-1}$	
ρ_w	Density of Water	1000	kg m^{-3}	
ρ_g	Density of Soil Layer	1700	kg m^{-3}	Adjustable
ρ_i	Density of Ice	917	kg m^{-3}	
ρ_s	Snow Density	50 to 500	kg m^{-3}	Adjustable
h_f	Heat of Fusion	333.5	kJ/kg	
h_v	Heat of Vaporization (ice to vapor)[1]	2834	kJ/kg	
A	Albedo	0.4 to 0.8		Adjustable
σ	Stefan Boltzmann Constant	2.0747 x 10^{-7}	kJ m^{-2} hr^{-1} K^{-4}	
ε_s	Emissivity of Snow	0.99		
T_r	Temperature above which precipitation is rain	3°C		Adjustable
T_b	Temperature below which precipitation is snow	-1°C		Adjustable
T_o	Temperature of Freezing	0°C		
P_{std}	Reference Atmospheric Pressure	101300	Pa	
T_{std}	Reference Atmospheric Temperature	20°C = 293K		
R_d	Dry Gas Constant	287	J kg^{-1} K^{-1}	
g	Gravitational Acceleration	9.81	m s^{-2}	
α	Reference Lapse Rate	0.0065	°C/m	Adjustable
a	Atmospheric Absorption Parameter	0.09		Adjustable
g_s	Atmospheric Absorption and Scattering Parameter	0.14		Adjustable
z_o	Snow Roughness Height	0.005	m	
z	Assumed Wind/Air Temperature Measurement Height	2	m	
D_e	Soil Effective Depth	0.4	m	Adjustable
k	Von Karmans Constant	0.4		
a	Kuz'min's Emissivity of Air Parameter	0.62		
b	Kuz'min's Emissivity of Air Parameter	0.005	$Pa^{-0.5}$	
L_c	Liquid Holding Capacity	0.05		Adjustable
K_{sat}	Snow Saturated Hydraulic Conductivity	160	m/hr	Adjustable
r_s	Snow Thermal Resistance	11 to 222	hr/m	Adjustable

Notes:

[1]Heat of vaporization is temperature dependent. We ignore this effect and use the value for 0°C.

Mass and Energy Balance Equations

Given the state variables U and W, their evolution in time is determined by solving energy and mass balance equations.

$$\frac{dU}{dt} = Q_{sn} + Q_{li}(T_a, RH, N) + Q_p(T_a, P) + Q_g - Q_{le}(T_S) + Q_h(T_S, T_a, V) + Q_e(T_S, T_a, V, RH) - Q_m(U, W) \quad (6)$$

$$\frac{dW}{dt} = P - M_r(U, W) - E(T_S, T_a, V, RH) \quad (7)$$

Terms in the energy balance equation (all in $kJ/m^2/hr$) are:

- Q_{sn} - net solar radiation
- Q_{li} - incoming longwave radiation
- Q_p - advected heat from precipitation
- Q_g - ground heat flux
- Q_{le} - outgoing longwave radiation
- Q_h - sensible heat flux
- Q_e - latent heat flux due to sublimation/condensation
- Q_m - advected heat removed by meltwater

Terms in the mass balance equation (all in m/hr of water equivalent) are:

- P - precipitation (rain and snow)
- M_r - meltwater outflow from the snowpack
- E - sublimation from the snowpack

Functional dependencies of these variables on driving and state variables are shown. We determine snowpack surface temperature T_S using a new equilibrium approach described below. This determines T_S from snowpack average temperature T determined from state variables U and W and surface energy flux functions. The parameterization for these are described below. Whenever possible, we have used physically sound parameterization, based on the process involved. Equation (6) and (7) form a coupled set of first order, nonlinear ordinary differential equations. They can be summarized as:

$$\frac{dU}{dt} = Q(U, W, \text{driving variables}) \quad (8)$$

$$\frac{dW}{dt} = F_m(U, W, \text{driving variables}) \quad (9)$$

or defining $\underline{X} = (U, W)$

$$\frac{d\underline{X}}{dt} = Q\, F_m(\underline{X}, \text{driving variables}) \tag{10}$$

In the current context with $\underline{X}$ specified initially, this is an initial value problem. A large variety of numerical techniques are available for solution of these equations [Gerald, 1978]. We currently use the second-order Euler Predictor - Corrector approach. This provides a satisfactory compromise between complexity and accuracy.

$$\underline{X}' = \underline{X}_i + \Delta t\, QF_m\,(\underline{X}_i, \text{driving variables}) \tag{11a}$$

$$\underline{X}_{i+1} = \underline{X}_i + \Delta t\, \frac{QF_m\,(\underline{X}_i, \text{driving variables}) + QF_m\,(\underline{X}', \text{driving variables})}{2} \tag{11b}$$

This is second order, with errors proportional to Δt^2.

Parameterization

Temperature - T. The snow and interacting soil layer average temperatures are obtained from the energy content and water equivalent, relative to 0°C ice phase. The heat capacity of the snow is $\rho_w\, W\, C_s$ [kJ/°C]. The heat capacity of the soil layer is $\rho_g\, D_e\, C_g$ [kJ/°C]. The heat capacity of liquid water is $\rho_w\, W\, C_w$. The heat required to melt all the snow water equivalent is $\rho_w\, W\, h_f$ [kJ]. See Table 1 for definition and values of the parameters. For $U < 0$, all water is frozen and

$$T = \frac{U}{\rho_w\, WC_s + \rho_g\, D_e\, C_g} \tag{12a}$$

For $0 < U < \rho_w\, W\, h_f$, there is a mixture of solid and liquid and

$$T = 0°C. \tag{12b}$$

For $U > \rho_w\, W\, h_f$, all the snow has melted and

$$T = \frac{U - \rho_w\, W\, h_f}{\rho_g\, D_e\, C_g + \rho_w\, W\, C_w} \tag{12c}$$

In practice, unless we allow ponded water (which we don't) W will always be 0 in (12c). However, W is retained in this expression for numerical consistency during time steps when the snowpack completely melts.

Heat flow in soil is governed by Laplace's equation. The depth of penetration of changes in surface temperature can be evaluated from the expression [Rosenberg, 1974]:

$$\frac{R_z}{R_s} = \exp\left(-z\left(\frac{\pi}{\alpha P}\right)^{\frac{1}{2}}\right) \tag{13}$$

where R_s is the range of temperature oscillation at the surface, R_z the range of temperature oscillation at depth z, P the period of oscillation, α the soils thermal conductivity parameter, typically in the range 0.004 to 0.006 cm^2/s.

Figure 8 shows that for oscillations less than one week, the effect at 40 cm is damped to less than 30% and even for monthly oscillations is still damped 50% at 40 cm depth. This suggests using D_e = 40 cm in our model. Soil above this depth will interact thermally with the snow at time scales of weeks to months. Rosenberg [1974] also suggests this as an effective depth.

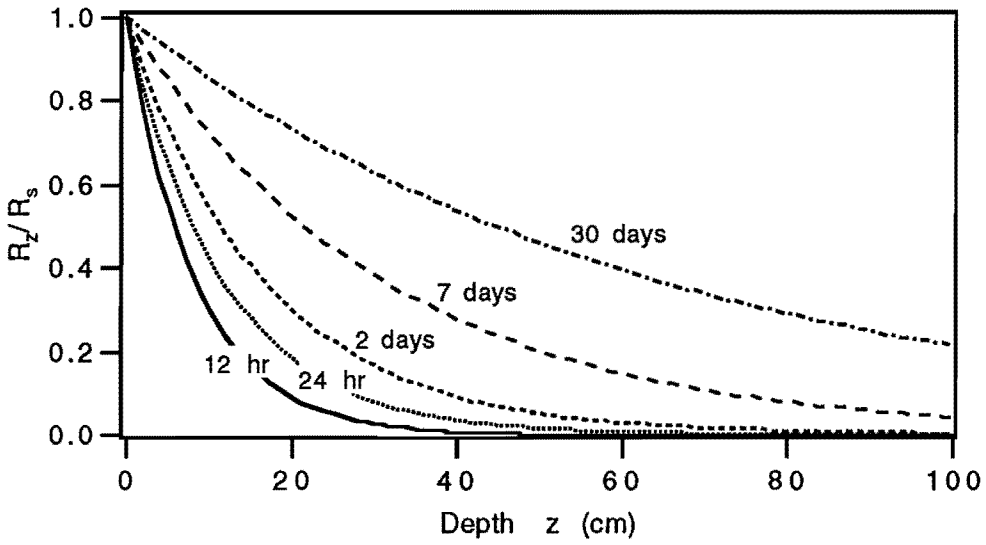

Figure 8. R_z/R_s vs. z for α = 0.005 cm^2/s for different durations.

Net Shortwave Radiation, Q_{sn}

This is calculated as

$$Q_{sn} = Q_{si}\,(1\text{-}A) \tag{14}$$

where A = albedo and Q_{si} is average incoming solar radiation.

Solar radiation incident on a horizontal surface is [Male and Gray, 1981]:

$$I_h = I_o \int_t^{t+\Delta t} \cos Z_s \, dt = I_o \, RF_h \tag{15}$$

where Z_s the solar zenith angle (angle between sun and vertical), I_o the solar constant (4914 KJ m^{-2} h^{-1}) and RF_h the horizontal radiation adjustment factor, calculated from orbital properties (accounting for season and latitude) by evaluating the integral in (15). Solar radiation incident on a sloping surface (without atmospheric effects) is similarly:

$$I_s = I_o \int_t^{t+\Delta t} \cos \psi \, dt = I_o \, RF_s \tag{16}$$

where ψ is angle between sun and surface normal (accounting for season, latitude, slope and aspect) and RF_s is the radiation adjustment factor accounting for slope and aspect.

Where cloud fraction N is not available a cloudiness factor CF is obtained from daily maximum temperature using empirical procedures given by Leavesley, et al. [1983].

The average flux, per unit horizontal area over Δt, modulated for cloudiness is:

$$Q_{si} = I_o \, CF \left(\int_t^{t+\Delta t} \cos \psi \, dt \right) / \Delta t \cos \theta = \frac{I_o \, RF_s \, CF}{\Delta t \cos \theta} \tag{17}$$

where θ is the slope.

When N is known we distinguish between direct and diffuse radiation using procedures adopted from Male and Gray [1981] and Bonan [1991].

Solar radiation incident on a horizontal surface attenuated for cloud and atmospheric absorption is

$$I_d = (1 - g_s) \, (1 - N)^{0.61} \, I_h \tag{18}$$

where g_s is an atmospheric absorption and scattering parameter and N is cloud fraction. The time averaged direct solar radiation per unit horizontal area, accounting for slope and aspect is then:

$$Q_d = I_d \frac{I_s}{I_h} / \Delta t \cos \theta = I_d \frac{RF_s}{RF_h} / \Delta t \cos \theta \tag{19}$$

The diffuse radiation flux [Male and Gray, 1981] is:

$$I_f = 0.5 \left[(1 - a) \, I_h - I_d \right] \tag{20}$$

where a is an atmospheric absorption parameter. This assumes that incident radiation, not absorbed or direct is scattered with 50% reaching the surface. Time averaged diffuse flux per unit horizontal area is then:

$$Q_f = I_f / \Delta t \cos\theta \tag{21}$$

Combining (19) and (21):

$$Q_{si} = Q_d + Q_f \tag{22}$$

This approach neglects the dependence of attenuation on the zenith angle (optical air mass) and dependence of albedo on angle of incidence. The parameter a, suggested value, 0.09 [Male and Gray, 1981] accounts for absorption by water vapor and ozone. The parameter g_s includes atmospheric absorption and scattering, so logically $g_s > a$. Bonan [1991] reports that it ranges from 0.08 to 0.67 and he calibrated $g_s = 0.14$ at Fairbanks.

Incoming Longwave Radiation, Q_{li}

Under clear skies (or where N is not known) incoming longwave radiation is

$$Q_{li} = \varepsilon_a \sigma T_a^4 \tag{23}$$

where ε_a is the effective emissity of the atmosphere, σ the Stefan Boltzmann constant and T_a, air temperature in Kelvin.

ε_a is, in general, a function of the vapour pressure distribution in the atmosphere. Several approximations in terms of surface vapor pressure e_a (in Pa) are available.

Brunt [1952]: $$\varepsilon_a = a + b\sqrt{e_a} \tag{24}$$

Kuz'min [1961] has suggested a = 0.62 and b = 0.005 $P_a^{-0.5}$.

Brutsaert [1975]: $$\varepsilon_a = 0.642 \left(\frac{e_a}{T_a}\right)^{\frac{1}{7}} \tag{25}$$

Satterlund [1979]: $$\varepsilon_a = 1.08 \left[1 - \exp\left(-\left(\frac{e_a}{100}\right)^{T_a/2016}\right)\right] \tag{26}$$

Male and Gray [1981] note that the Satterlund formula compared better than the Brutsaert formula against measurements at temperatures below 0°C. Marks and Dozier [1979] suggest adjusting the Brutsaert [1975] formula for elevation, since it was derived for sea level conditions. They use:

$$T' = T_a + 0.0065\ z \tag{27a}$$

$$e' = \frac{e_a}{e_s(T_a)} e_s(T') \tag{27b}$$

as equivalent sea level temperature and vapour pressure.

Then

$$\varepsilon_a = 0.642 \left(\frac{e'}{T'}\right)^{\frac{1}{7}} \frac{P_a}{P_{std}} \tag{27c}$$

where P_a is the air pressure estimated from elevation, according to equation (36) below.

We currently use the Satterlund formula. Future work will evaluate or incorporate the other options. Under cloudy skies incoming radiation from the clouds (assumed to be black bodies) is

$$Q_{li\ clouds} = \sigma T_c^4 \tag{28}$$

Then

$$Q_{li} = N\, Q_{li\ clouds} + (1 - N)\, Q_{li\ clear} \tag{29}$$

The temperature of the cloud base is obtained by assuming a lapse rate (α = 0.0065 °c/m) and cloud height (1000 m) unless this information is known.

Outgoing Longwave Radiation, Q_{le}

Snow is essentially a black body, with $\varepsilon_s \approx 0.99$. Outgoing radiation is

$$Q_{le} = \varepsilon_s \sigma T_s^4 \tag{30}$$

Heat with Precipitation, Q_p

The partitioning between rain and snow is based on air temperature, according to Figure 9.

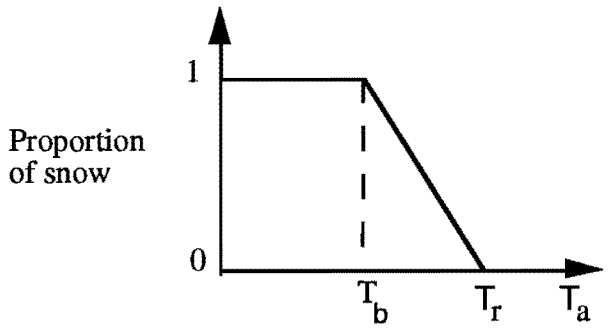

Figure 9. Temperature criteria used to divide precipitation into rain and snow [Bowles et al., 1975].

$$P_S = P \text{ if } T_a < T_b$$

$$= P\frac{T_r - T_a}{T_r - T_b} \text{ if } T_b < T_a < T_r$$

$$= 0 \text{ if } T_a > T_r \tag{31}$$

$$P_r = P - P_s$$

This assumes snow for $T_a < T_b = -1°C$, rain for $T_a > T_r = 3°C$ and a mixture of snow and rain for air temperatures between T_r and T_b.

Precipitation is assumed to be at the air temperature, unless this is physically impossible (snow with $T_a > 0°C$). The advected heat is the energy required to convert this precipitation to the reference state (0°C ice phase).

$$Q_p = P_s \left(\text{Min}\left(T_a,\ 0°C\right) - 0°C \right) C_s \rho_w$$

$$+ P_r \left[h_f \rho_w + C_w \rho_w \left(\text{Max}\left(T_a, 0°C\right) - 0°C \right) \right] \tag{32}$$

Turbulent Fluxes, Q_h, Q_e, E

The concept of aerodynamic resistance and flux proportional to temperature and vapor pressure differences is used.

Considering a unit volume of air the heat content is $\rho_a C_P T_a$ and the vapor content $\rho_a q$, where ρ_a is air density, C_P air heat capacity, T_a air temperature and q, specific humidity. Heat transport towards the surface is given by

$$Q_h = \rho_a C_p (T_a - T_s)/r_a \quad \left[kJ\ m^{-2}\ s^{-1}\right] \tag{33}$$

where T_s is the surface temperature and r_a aerodynamic resistance. Vapor transport away from the surface (sublimation) is:

$$M_e = \rho_a (q_s - q)/r_a \quad \left[kJ\ m^{-2}\ s^{-1}\right] \tag{34}$$

where q_s is the surface specific humidity.

By comparison with the usual expressions for turbulent transfer in a logarithmic boundary layer profile [Male and Gray, 1981; Anderson, 1976; Brutsaert, 1982; Calder, 1990] for stable conditions one gets

$$\frac{1}{r_a} = \frac{k^2 V}{\left[\ln(z/z_o)\right]^2} \tag{35}$$

where V is the wind speed at height z, z_o is the "roughness height" at which the logarithmic boundary layer profile predicts zero velocity and k is von Karman's constant (0.4).

Future work will evaluate modifications to this that allow for effects of stability/instability in the boundary layer [Brutsaert, 1982], as well as the effect of a vegetation canopy [Bonan, 1991].

Application of (33) and (34) requires ρ_a, related to atmospheric pressure, P_a. We assume the following standard atmospheric approximation to give P_a as a function of elevation z,

$$P_a = P_{std} \left(\frac{T_{std} - \alpha z}{T_{std}} \right)^{\frac{g}{R_d \alpha}} \tag{36}$$

adapted from Marks and Dozier [1979],

where

P_{std} = Reference atmospheric pressure, 101300 Pa
T_{std} = Reference atmospheric temperature, 20°C = 293 K
α = Lapse rate = 0.0065 °C/m
R_d = Dry gas constant, 287 J kg^{-1} K^{-1}
g = Gravitational acceleration, 9.81 m/s^2

Then the ideal gas law is used to give

$$\rho_a = \frac{P_a}{R_d T_a} \tag{37}$$

We neglect the effect of water vapor on R_d. In solving (34) it is more convenient to work with vapor pressure, e_a, than specific humidity, using

$$q = \frac{0.622\, e_a}{P_a} \tag{38}$$

Recognizing that the latent heat flux towards the snow is

$$Q_e = - h_v M_e \tag{39}$$

with Equations (34), (38), and (39), one gets:

$$Q_e = \frac{h_v\, 0.622}{R_d T_a} (e_a - e_s)/r_a \tag{40}$$

where e_s is the surface vapour pressure. Over snow we assume this is saturated at the snow surface temperature T_s and use the following approximation [Chow et al., 1988].

$$e_s (T_s) = 611 \exp\left(\frac{17.27\, T_s}{237.3 + T_s}\right)$$

in Pa, for T_s in °C. Then the water equivalent depth of evaporation/sublimation is

$$E = - \frac{Q_e}{\rho_w h_v} \tag{41}$$

Snow Surface Temperature, T_s

Since snow is a relatively good insulator, it is more reasonable to use snow surface temperature, T_s rather than snowpack average temperature, T to compute the surface heat fluxes. To take this into account we developed a new approach to calculate T_s assuming equilibrium condition in the surface layer analogous to the Penman approach for calculating evaporation.

Heat conduction into/out of the snow is calculated using the temperature gradient and thermal diffusivity of snow. The governing equation is:

$$Q = -\kappa \rho_s C_s \frac{dT}{dZ} \tag{42}$$

Where,

κ = snow thermal diffusivity [m/hr]
ρ_s = snow density [kg/m^3]
C_s = ice heat capacity [KJ/kg/°C]

This is approximated by:

$$Q = -\kappa \rho_s C_s \frac{T - T_s}{Z_e} \tag{43}$$

Where,

T = average temperature of snowpack [°C]
T_s = snow surface temperature [°C]

and Z_e is an effective depth over which this thermal gradient acts. The factor Z_e/κ is denoted r_s, snow thermal resistance, analogous to aerodynamic resistance, r_a. Equation (26) can then be written as:

$$Q = \rho_s C_s \frac{(T_s - T)}{r_s} \tag{44}$$

This calculates heat flux as a product of the temperature difference between the snow surface and average. A value of r_s is obtained by assuming a depth, Z_e equal to the depth of penetration of a diurnal temperature fluctuation calculated from equation (13) [Rosenberg, 1974]. Z_e is chosen so that R_z/R_s is small (here taken rather arbitrarily as 1/e). In fact r_s is used as a tuning parameter, with this calculation used to define a reasonable range. Then assuming equilibrium at the surface, the surface energy balance gives.

$$Q = Q_{sn} + Q_{li} + Q_h + Q_e + Q_p - Q_{le} \tag{45}$$

Surface temperature dependent fluxes are:

$$Q_h(T_s) = \frac{\rho_a C_P}{r_a}(T_a - T_s) \tag{46}$$

$$Q_e(T_s) = -\frac{h_v \rho_a}{r_a}\{q_s(T_s) - q_a\} \tag{47}$$

$$Q_{le}(T_s) = \varepsilon_s \sigma T_s^4 \tag{48}$$

Q_{sn},Q_{li} and Q_p may be regarded as prescribed inputs. Equations (44) to (48) have unknowns Q, T_s, Q_h, Q_e, Q_{le} with inputs T, T_a, q_a, Q_{sn}, Q_{li}.

Analogously to the Penman approach they can be solved by linearizing T_s about a reference temperature, T_*. Penman used $T_* = T_a$. This gives

$$Q_e = \frac{h_v \rho_a}{r_a}\left\{q_s(T_s) + \frac{dq_s}{dT}(T_s - T_*) - q_a\right\} \tag{49}$$

Now with $q = \frac{0.622 e_a}{P_a}$ and denoting $\frac{de_s}{dT} = \Delta$, we have

$$Q_e = -\frac{h_v \rho_a}{r_a}\frac{0.622}{P_a}\left\{e_s(T_*) + \Delta(T_s - T_*) - e_a\right\} \tag{50}$$

Similarly, linearizing the outgoing longwave radiation, equation (48), one gets:

$$Q_{le} = \varepsilon_s \sigma T_*^4 + 4\varepsilon_s \sigma T_*^3 (T_s - T_*) \tag{51}$$

Substituting these into (45) we get:

$$\begin{aligned}\frac{\rho_s C_s}{r_s}(T_s - T) = {} & Q_{sn} + Q_{li} + Q_p + \frac{\rho_a C_p}{r_a}(T_a - T_s) \\ & - \frac{h_v \rho_a}{r_a}\frac{0.622}{P}\left\{e_s(T_*) + \Delta(T_s - T_*) - e_a\right\} \\ & - \varepsilon_s \sigma T_*^4 - 4\varepsilon_s \sigma T_*^3 (T_s - T_*)\end{aligned} \tag{52}$$

Solving for T_S gives:

$$T_s = \frac{Q_{sn} + Q_{li} + Q_p + \frac{T_a \rho_a C_P}{r_a} - \frac{0.622 h_v \rho_a}{r P}\left\{e_s(T_*) - e_a - \Delta T_*\right\} + 3\varepsilon_s \sigma T_*^4 + \frac{\rho_s C_s T}{r_s}}{\frac{\rho_s C_s}{r_s} + \frac{\rho_a C_P}{r_a} + \Delta\frac{h_v \rho_a}{r_a}\frac{0.622}{P} + 4\varepsilon_s \sigma T_*^3} \tag{53}$$

If this T_s is significantly different from T_*, T_* should be replaced by T_s and the procedure iterated. The procedure converges rapidly to a final T_s which if less than freezing is used to calculate surface

energy fluxes. If the final T_s is greater than freezing it means that the energy input to the snow surface cannot be balanced by thermal conduction into the snow. Surface melt will occur and the infiltration of meltwater will account for the energy difference and T_s is then set to 0°C.

Meltwater Outflux, M_r and Q_m

The energy content state variable determines the liquid content of the snowpack. This, together with Darcy's law, is used to determine the outflow rate.

The water equivalent depth of liquid water in the snow is $U/h_f \rho_w$. L_f denotes the fraction of total snowpack (liquid and ice) that is liquid,

$$L_f = \frac{U}{\rho_w h_f W} \tag{54}$$

The solid fraction is then $1 - L_f$.

Now we assume that the solid fraction supports the matrix with a solid matrix density ρ_S. Given the density of ice and density of water one can calculate the pore volume and water filled pore volume. Our model of snow drainage assumes an initial capillary holding capacity, a fraction L_c (0.05) of the solid matrix water equivalent. Liquid above this holding capacity is free to flow according to Darcy's Law with an assumed unit head gradient due to gravity.

Male and Gray [1981] suggest hydraulic conductivity.

$$K_s = \frac{\rho_w g k}{\mu} S^{*3} \tag{55}$$

where k = intrinsic permeability, μ = viscosity, and S* is the relative saturation in excess of water retained by capillary forces.

$$S^* = \frac{\text{liquid water volume - capillary retention}}{\text{pore volume - capillary retention}} \tag{56}$$

Volume calculations yield:

$$S^* = \left(\frac{L_f}{1 - L_f} - L_c \right) / \left(\frac{\rho_w}{\rho_s} - \frac{\rho_w}{\rho_i} - L_c \right) \tag{57}$$

where ρ_i is the density of ice (917 kg/m^3). Define the constants in (55) as K_{sat}. Our model for melt outflux is then

$$M_r = K_{sat} S^{*3} \tag{58}$$

with S* from (57) and K_{sat} a parameter (160 m/hr based on typical values from Male and Gray [1981]).

This melt outflow is assumed to be at 0°C so the heat advected with it, relative to the solid reference state is:

$$Q_m = \rho_w h_f M_r \tag{59}$$

Our results have shown that this parameterization of melt outflow is capable of modeling continued outflow from a ripe snowpack even after the net energy exchange has become negative. This agrees with observations.

Results

Some of the parameters in the model described above have uncertain values. In particular, albedo has a range from 0.8 for fresh snow to 0.4 for old dirty snow [Bowles et al., 1975]. Snow thermal resistance, r_s depends on density and assumed effective depth and realistic bounds on this we calculated as 11 to 222 hr/m. Snow density, ρ_s varies in the range of 50 to 500 kg/m^3. Ground heat flux is typically small with values in the range of 0 to 50 kJ/m^2/hr [Male and Gray, 1981]. There is also uncertainty in snow saturated hydraulic conductivity, K_{sat} and liquid holding capacity, L_c although melt delivery rates are not very sensitive to these. We have not yet tested the model on Data from Reynolds creek. Figure 10 shows a comparison of model and observed water equivalent using data collected at the Central Sierra Snow Laboratory. In making this comparison we have adjusted albedo, r_s and Q_g within their reasonable limits to obtain a fit between modeled and observed values of snow water equivalent, melt outflow and radiation. Table 3 shows the list of parameters with their lower and upper bound and the parameter values which the model currently uses.

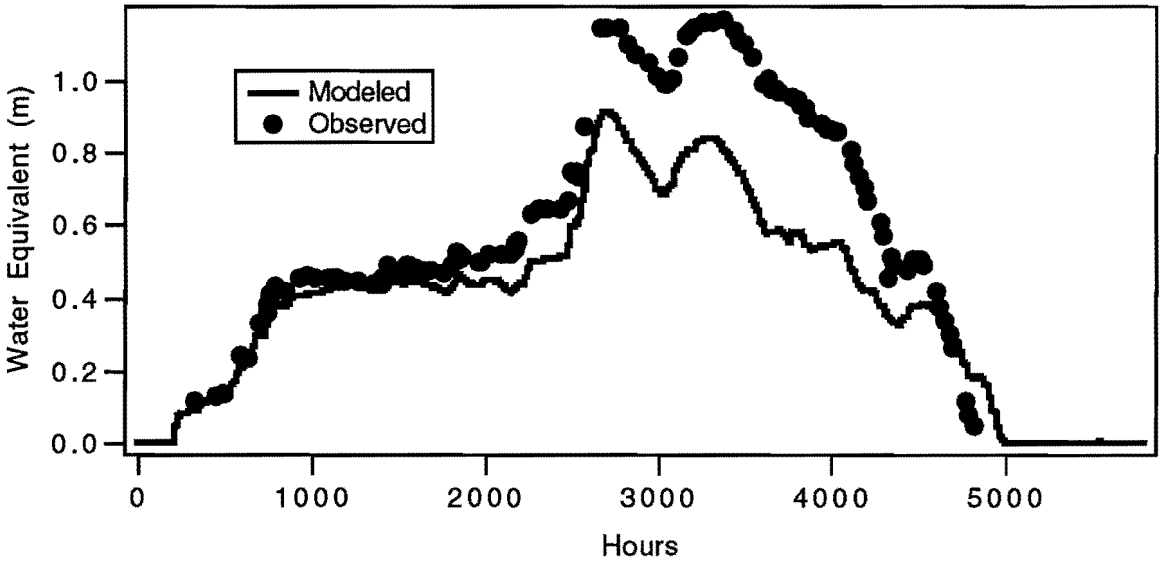

Figure 10. Comparison of modeled and observed water equivalent. Data from Central Sierra Snow Laboratory, 1985/1986 winter.

Table 3. Parameters adjusted to achieve fit to data.

Parameters	Lower Bound	Upper Bound	Value Used
Albedo, A	0.4	0.8	0.6
Snow Thermal Resistance, r_s (hr/m)	11	222	30
Ground Heat Flux, Q_g (kJ/m^2/hr)	0	50	50
Density of Snow, ρ_s (kg/m^3)	50	500	450

Isotope/Process Hydrology Studies

Although the 1992 field season at Upper Sheep Creek was necessarily postponed, several other sub-objectives were addressed within the guidelines of the original USGS proposal framework. The following pages outline isotope work completed during year 1, as a prelude to the main field campaign in March-August 1993.

The Central Sierra Snow Lab Snowcover Isotope Fraction Study

Rationale

Isotopes of hydrogen ($^2H \equiv D$) and oxygen (^{18}O) have been used extensively in watershed hydrology over the past two decades [Sklash and Farvolden, 1979; Kennedy et al., 1986]. Most of these investigations have been undertaken in humid temperate regions, excluding the effect of season snowcovers on isotope-hydrologic relationships. Recent studies have suggested that assumptions associated with the technique may limit its applicability under many circumstances [Rodhe, 1987]. Under temperate rainfall-dominated conditions, for example, McDonnell et al. [1990] have shown that rainfall ΔD and $\Delta^{18}O$ may vary both spatially and temporally during an event, complicating simple two component hydrograph separations commonly used. Kendall and Gu [1991] and McDonnell et al. [1991] have shown that soil water and groundwater concentrations may also vary widely in time and space, even within relatively small homogeneous watersheds.

Under snow-dominated conditions, much less is known about ΔD and $\Delta^{18}O$ variations during the melt period [Rodhe, 1987; Moore, 1989]. Notwithstanding, there is considerable interest in applying principles of isotope hydrology to many northern and alpine hydrologic regimes. In addition to tracing water movement in and out of the snowpack, isotope tracing can be valuable for determining the residence time of water in different layers and water transport in both liquid and gaseous phases. Isotope analysis also provides a unique way of quantifying evaporation from a melting snow cover.

In Europe, early studies by Dincer et al. [1970] documented the oxygen-18 content in snow. They showed that evolution of the isotopic composition of the snowpack reflects the movement of meltwater in the snowpack and its relation to the thermal condition in the pack. Early snowmelt was seen to percolate through the snowpack without much mixing with the snow matrix. At the middle of the snowmelt period, the meltwater mixed with the water in the lower layers during the

percolation of water through the snowpack. Dincer et al. [1970] described a pseudo-altitude effect in the snowpack due to the disappearance of the isotopically light early winter snow from the lower altitudes which are subject to intermittent melting during the winter months.

Stichler et al. [1987] found that isotope concentrations varied in respective snow layers, indicating a mass exchange between the percolating melt water and the snowpack. A correlation was found between the isotope concentrations in the snowpack and in the melt water. Herrmann et al.[1981] conducted several cold room experiments with isotopically homogeneous and stratified snow columns, to study the effects of isotope fractionation and exchange processes in the snow cover on the isotopic melt concentrations. Alternations of the melt intensities caused marked variations of the isotopic contents of the snowpack outflows. Herrmann et al.[1981] noted that the difference between the deuterium contents of the surface layer, where the initial melt water is produced, and that of the outflow was very small.

In North America, early studies by Friedman and Smith [1972] and Meiman et al. [1974] examined the isotopic composition of Rocky Mountain snowpacks as an index to winter climate.

The objectives of this present research is to examine the isotopic composition of snow and meltwater infiltration at the USDA Central Sierra Snow Lab in order to address the following questions: (1) what effect does strong boundary layer sensible and latent heat flux have on the net isotopic flux in snow; (2) can the meltwater isotopic composition be predicted based on isotopic changes in the snowpack; and (3) what is the extent of vertical isotopic layering of the snowpack? Snow energy balance and flow path analysis will also be conducted during periods of active melt and related to changes in isotopic composition of precipitation, snow stratigraphy and melt.

Early Isotope Studies at Central Sierra Snow Lab

Snow research at the Central Sierra Snow Lab has been on-going for the past 45 years. In addition to basic hydrological and physical snow studies, some preliminary isotopic research has been undertaken. Krouse and Smith [1972] examined $^{18}O/^{16}/O$ abundances in a seasonal snowpack at the site and found that snow $\Delta^{18}O$ values ranged from -5 to -26 $^{0}/OO$. Isotopic composition of snow layers was related to air temperature and wind direction and changed markedly as melt water moved through the pack. Samples collected by Krouse and Smith [1972] bore no simple relationship to temperature or any other meteorological parameters. Marked strata in the snowpack did not retain its isotopic composition throughout the winter season. In terms of snow isotopic-stratigraphy relations, Krouse and Smith [1972] found that water may be preferentially retained in a layer and become permanently identified with the layer, or water may move through with little retention or interaction. Therefore, water movement in the pack may increase or decrease the $\Delta^{18}O$ content of a particular stratum, with the change being transient or persistent for long time. This non-linear effect identified at the CSSL makes both isotope hydrologic tracing (and inferences to paleoclimatic reconstruction) highly problematic.

An additional set of study objectives will relate directly to the Krouse and Smith [1972] work: (1) to replicate and understand the physics behind the rather confusing results of Krouse and Smith [1972], and (2) to look at longer term temporal variability of snow isotopic composition by comparing 1991/92 data with those reported for the 1965-68 period by Krouse and Smith [1972].

Study Site and Instrumentation

The research utilized the Central Sierra Snow Laboratory (CSSL), located at 2100 m elevation 25 km northwest of Lake Tahoe, California. The site is situated on the western slope of the Sierra Nevada and is strongly influenced by maritime air masses which result in deep snow accumulation through the winter months. Snow comprises about 85% of the annual precipitation with peak accumulation from January through March. An average peak snow depth of 3050 mm and snow water equivalent of 900 mm is reached by early April.

The CSSL facility is maintained by the USDA/Forest Service Pacific Southwest Experiment Station. The primary measurement site is a forest clearing covering roughly 4000 m^2 surrounded by mature lodgepole pine forest. Complete energy balance instrumentation are present for monitoring radiative and turbulent fluxes. In addition, snowpack liquid water release (basal outflow) is monitored (and sampled) using an array of lysimeters installed at the soil surface, covering roughly 50 m^2. The timing and amount of basal outflow induced by in situ melt and rain-on-snow are monitored continuously for each of the dozen pans by tipping bucket mechanisms.

Sampling Strategy

Physical measurements included hourly values of net radiation, shortwave radiation up and down, delta temperature, delta relative humidity, windspeed (preferably at least two heights), precipitation intensity, and snow temperature (if possible). These measurements were achieved using pre-existing electronic instrumentation at the site. In addition, a number of manual physical snow measurements were made for the study. These included pit observations of grain size (by layer), along with layer density, liquid water content and thickness. Most of these in-situ measurements will be obtained in the main measurement area (a clearing), at a resolution of around 10 mm.

Approximately 2000 snow and water samples were collected during the study. Approximately 1500 snowmelt samples (without replication) were collected from the base of the snowpack. Roughly 50 precipitation samples (both snow and rain) were collected for individual storms, plus approximately 500 layer-specific snow pit samples (without replication).

Precipitation

Snowfall during the 1991/92 winter season was collected for each event. A bulk 1x1 m snow board sample was bagged and melted following the sampling protocol outlined below. Rainfall was simply bulk collected in a raingauge and poured into sample vials. No attempt was made to determine the sequential isotopic composition of rain or snow.

Snowpack

Concurrent with the in-situ measurements and pit observations of layer grain size, density, liquid water content and thickness, samples were extracted for layer-specific isotopic analysis. A new pit was dug for each sample collection to minimize evaporative effects from an exposed "face". It was expected that little spatial variability would be encountered over a distance of tens of meters, therefore, the excavation of new pits in and around the main measurement was not be a problem.

Snowpack layer samples were obtained at 100 mm increments within the snowpack, once the pack had become isothermal. Prior to snowpack "ripening", layers that were easily "trackable" to specific precipitation events were also sampled. Layer-specific samples were collected weekly during the accumulation phase and then daily during active melt. In addition, snow layers during rain-on-snow events (on either a cold or isothermal snowpack) were sampled at least daily, or

more frequently if manpower permitted. Mid-winter thaws were be sampled daily, as per melt season sampling.

Melt Water

Melt water from the base of the snowpack was collected daily during active melt, rain-on-snow or periodic thaws. Ideally, a composite sample was obtained for the daily melt volume. This sample was mixed in a sealed container and a 20 ml sample was retained for subsequent isotopic analysis. For rain-on-snow events, and for three individual melt events (early, middle and late parts of the melt cycle), hourly samples were collected in addition to the daily composite sample. This was achieved via grab samples as the technician's schedule permitted.

Sampling Protocol

The procedure for collection of snow water samples was to: (1) collect the snow sample in a large sealable jar or ziplock baggie, (2) bring the sealed sample indoors and allow it to melt. Once the sample had melted, water was poured into 20ml bottle so the bottle is completely full with no air remaining, (3) the labelled bottles were then stored at room temperature, until the time it was shipped out to the USGS Menlo Park Water Resources isotope lab.

Research Schedule

The research and data collection at the CSSL ran from November 1991 until the snow was absent in June 1993. Drs. Neil Berg and Bruce McGurk of the U.S. Forest Service supervised all data collection carried out by two full-time USDA/FS technicians at the CSSL site. Dr. Carol Kendall of the USGS Menlo Park, Water Resources Division is now conducting the mass spectrometer analyses for ΔD and $\Delta^{18}O$ concentrations of collected water samples.

Relevance to the Reynold's Creek Distributed Water Balance Model

Objective 1: What effect does strong boundary layer sensible and latent heat flux have on the net isotopic flux in snow?

Relevance: Advection of sensible and latent heat onto the main drift area at Upper Sheep Creek is thought to control melt to a large extent. Isotope fractionation within the pack, therefore, becomes a major concern in terms of affecting the isotope input to the local groundwater system.

The energy balance data will be used to estimate ablation (sublimation and/or melt) during both melting and non-melting periods. By determining the radiative, sensible and latent heat fluxes at the snow surface boundary layer, measurements of net isotopic flux from the atmosphere can be compared mass and vapor flux information. These relationships will then be generalized to easily measured weather variables. Both principal components analysis and stepwise multiple liner regression analysis will be used.

Objective 2: Can the meltwater isotopic composition be predicted based on isotopic changes in the snowpack?

Relevance: The main snow drift at Upper Sheep Creek is roughly 10 m deep in normal snow years. This extreme depth and amount of effort and and samples required to address Objective 2 makes it impossible to treat within the realm of the USGS project. Nevertheless, this question is of vital importance to the modeling of the isotope water balance. Theoretically, the data and interpretations from CSSL should apply in this case.

The meltwater emanating from the base of the snowpack may be either enriched or depleted as compared to the snowpack. Isotopic variations in the daily composite melt sample will be related to the actual melt rate and volume measurements. The degree and rate of snowpack isotopic homogenization through melt will be related to melt isotopic composition. This leads into objective 3.

Objective 3: What is the extent of vertical isotopic layering of the snowpack?

Relevance: Once again, the extreme depth of the Upper Sheep Creek drift prevent this question from being fully resolved. It is expected that condensation and evaporation at the snow surface, combined with diffusion and convection processes within the snow itself, may enrich the isotope composition of the pack. As the melt progresses, homogenization of the pack will occur. The timing of this homogenization will be important to understand for sampling design and computing well lag response from the melt input.

A chief factor in determining the isotopic composition of meltwater is the isotopic layering of snowpack. In the deep CSSL snowpack, deposited at both cold and relatively warm temperatures, there will be a sequence of high delta oxygen-18 (reflecting cold temperature snowfall conditions) and low delta oxygen-18 (reflecting warmer snowfall conditions). Also, since the pack is quite deep, a high delta oxygen-18 water melting from the surface layer at the beginning of melt for example, may be reduced by isotopic exchange during percolation, and the draining meltwater at the base of the pack may be depleted in oxygen-18 as compared with the snowpack.

General Implications

Watershed hydrologic modelling requires accurate portrayal of the input of hydrologic components in the snowmelt hydrograph. Data collected in this project should help in improve understanding of temporal variation of the input function on simple mass balance models and for more sophisticated numerical techniques.

Field Activities at Upper Sheep Creek

Installation of Suction Lysimeters and Soil Moisture Instrument Installation

Two transacts of low volume 1 bar suction lysimeters were installed at Upper Sheep Creek. One transect included SL's spaced at 30 m intervals downslope from the main drift, the other positioned normal to the slope, immediately downslope from the drift.

Neutron probe access tubes were installed on two transects in the north facing side of Upper Sheep creek. Gravimetric samples were taken at different depths during installation to calibrate the probes. The installed neutron access tubes will supplement the access tubes previously installed by the USDA-ARS. Soil moisture measurements will be taken weekly using the neutron probe for the north facing side and using the gravimetric method in the south facing side during the field data collection period.

Sampling of Piezometers

All piezometers were sampled at three separate times throughout the 1991/92 season, in order to obtain baseline isotope data.

Establishment of a Local Meteoric Water Line

Commencing March 1992, all rainfall and snowfall events were sampled at the Reynold's Creek quonset. These samples were, and will continue to be, collected by ARS technical staff, in order to characterize the local isotopic meteoric water line (MWL). This MWL is the relationship between deuterium and oxygen-18 and is important for relating samples obtained during the melt to possible evaporative effects en route to groundwater recharge.

Development of an Isotopic Mass Balance Within the TOPMODEL Framework

In addition to those modelling approaches outlined in the original proposal, new attempts have been made in year 1 to better incorporate the isotope tracing campaign with the distributed modeling approach. As stated earlier in this report, the mass balance for a pixel P with multiple-direction input and output is given by:

$$\sum_{i=1}^{n} q_{ip} - \sum_{j=1}^{m} q_{jp} - ET_p + M_p = \frac{d(nz)}{dt} \tag{60}$$

The isotopic mass balance is given by

$$\sum_{i=1}^{n} q_{ip}\,\delta_{ip} - \sum_{j=1}^{m} q_{jp}\,\delta_{jp} - ET_p\,\delta_{ETp} + M_p\,\delta_{Mp} = \frac{d(nz\delta)}{dt} \tag{61}$$

Here
- n = number of contributing pixels
- m = number of pixels to which flow takes place from P
- q_{ip} = flow from pixels i to P
- ET_p = evapotranspiration loss from pixel P
- M_p = snowmelt input to P
- n = effective porosity
- δ_{ip} = isotopic signature of flow from i to P
- δ_{ETp} = isotopic signature of the evaporative flux from P
- δ_{Mp} = isotopic signature of snowmelt input into P

It will be assumed that there is complete mixing of all inflows in P before the water flows out of it ($\delta_{jp} = \delta_{outp}$). The evaporative flux may be considered negligible during the early melt season. The above equations will be applied along select transacts with indications of prominent water movement from the piezometer data. When a balance is achieved, the area of application will be increased by introducing more pixels into the analysis.

Spatial Analysis of Piezometric Data

In an effort to develop a conceptual model for flow in this basin Flerchinger et al [1992] obtained lagged spatial cross-correlations between different piezometer levels. They drew inferences of groundwater residence times and obtained some idea of the flow paths in the basin. The study was conducted for 1986 and 1987. The former was a normal precipitation year and the latter, a dry year. There were significant differences in the basin response for the two years.

Results obtained by the above methods of isotopic mass balance and solutions to the convective-dispersive equation will give the spatial and temporal variations of isotope concentrations. A lagged cross-correlation analysis of piezometer levels will also be conducted and the results compared against the isotope concentrations to determine the flow paths in a robust fashion. The lagged cross-correlation between piezometers x and y for lag k is given by

$$\rho_{xy}(k) = \frac{\sum_{t=1}^{n-k} (x_t - \bar{x})(y_{t+k} - \bar{y})}{\sqrt{\sum_{i=1}^{n} (x_t - \bar{x})^2} \sqrt{\sum_{i=1}^{n} (y_t - \bar{y})^2}} \qquad (62)$$

Airborne Videography and Evapotranspiration Studies

Video images of Reynolds Creek experimental watershed were collected using the USU airborne multispectral video/radiometer system [Neale, 1991] consisting of three video cameras, four band EXOTECH radiometer and thermal infrared radiometer. Overflights were made on June 20 and July 27 1992 that covered both the Upper Sheep creek and Reynolds mountain sub-catchment. The video data were taken from a flight altitude of 3560 m above sea level, which was 1524 - 1720 m above the ground surface. This flight altitude with 16 millimeter camera lens at focal aperture of 8 resulted in pixel sizes of about 2 m. The data was collected under relatively clear sky conditions. Video images on each spectral band tape were digitized with a 386-PC computer that has a frame grabbing board (TARGA+) and software to convert the images into an ERDAS compatible format. The Earth Resource Data Analysis System (ERDAS) software was then used to register and stitch images together.

At time of the overflight of June 20 irradiance data were collected over a calibrated standard barium sulphate reflectance panel located at the center of Upper sheep creek sub-basin. The irradiance data was used to transform the radiance data to reflectance. Also coincident with the June 20 overflight a ground based four band EXOTECH radiometer was used to measure Canopy reflectance along four transacts in the Upper Sheep Creek subbasin. On some transects the canopy radiometric temperature was measured using an EVEREST infrared radiometer (8 - 14 fm).

From June 19 to 21 (before during and after the June 20 overflight) filed based evapotranspiration measurements were made. Latent heat flux data were collected with Campbell Scientific Bowen ratio energy balance systems (BREB) and eddy correlation system (ECRS). At Upper Sheep creek two ECRS were used, one on each of the north facing and south facing sides. At Reynolds mountain sub-catchment one BREB and one ECRS were used. A tower with four Young cup anemometers was used to determine the wind profile that is used to determine the zero plane displacement and the roughness height. This data will be used to relate evapotranspiration fluxes to video reflectances.

One of the uses of the video images is mapping of vegetation types. Unsupervised classification techniques were applied to the video images to cluster the spectral signatures of the images into classes corresponding to the vegetation types (forest, shrub, grassland, bare soil and mixed classes) present. Figure 11 gives an example of this classification.

Figure 11. Unsupervised classification of portion of Reynolds Creek Overflight data.

References

Anderson, E. A., (1976), "A Point Energy and Mass Balance Model of a Snow Cover," NOAA Technical Report NWS 19, U.S. Department of Commerce.

Bonan, G. B., (1991), "A Biophysical Surface Energy Budget Analysis of Soil Temperature in the Boreal Forests of Interior Alaska," Water Resources Research, 27(5): 767-781.

Bowles, D. S., J. P. Riley and G. B. Shih, (1975), "An Application of the Utah State University Watershed Simulation Model to the Entiat Experimental Watershed, Washington State," Report No. PRWG126, Utah Water Research Laboratory.

Brunt, D., (1952), Physical and Dynamical Meteorology, Cambridge University Press, Cambridge.

Brutsaert, W., (1975), "On a Deriveable Formula for Long-Wave Radiation from Clear Skies," Water Resources Research, 11: 742-744.

Brutsaert, W., (1982), Evaporation into the Atmosphere, Kluwer Academic Publishers, 299 p.

Calder, I. R., (1990), Evaporation in the Uplands, John Wiley & Sons.

Chow, V. T., D. R. Maidment and L. W. Mays, (1988), Applied Hydrology, McGraw Hill, 572 p.

Dincer, T., J. Martinec, B. R. Payne and C. K. Yen, (1970),"Variation of the Tritium and Oxygen-18 Content in Precipitation and Snowpack in a Representative Basin in Czechoslovakia.," Isotope Hydrology 1970. Proc. Symp. of IAEA, Vienna, 23-42.

Flerchinger, G. N., C. K. R and R. D. R, (1992), "Groundwater Response to Snowmelt in a Mountainous Watershed," J. Hydrol., 133: 293-311.

Friedman, I. and G. I. Smith, (1972), "Deuterium Content of Snow as an Index to Winter Climate in the Sierra Nevada Area," Science, 176: 790-793.

Gerald, C. F., (1978), Applied Numerical Analysis 2nd ed.

Herrmann, A., M. Lehrer and W. Stichler, (1981), "Isotope Input into Runoff Systems from Melting Snow Covers," Nordic Hydrology, 12: 309-318.

Kendall, C. and W. Gu, (1991),"Development of Isotopically Heterogenous Infiltration Waters in an Artificial Catchment in Chuzhou, China," Proc. Int. Symp. on the Use of Isotopic Tech. In Water Resources, IAEA, Vienna, 13.

Kennedy, V. C., C. Kendall, G. W. Zellweger, T. A. Wyermann and R. A. Avanzino, (1986), "Determination of the Components of Stormflow Using Water Chemistry and Environmental Isotopes, Matolle River Basin, California," J. Hydrol., 84: 107-140.

Krouse, H. R. and J. L. Smith, (1972),"O18/O16 Abundance Variations in Sierra Nevada Seasonal Snowpacks and Their Use in Hydrologic Research.," Proc. Int. Hydrol. Decade Snow and Ice Symposium, Banff, Canada, 24-38.

Kuz'min, P. P., (1961), Protsess Tayaniya Shezhnogo Pokrova (Melting of Snow Cover), [English translation by Israel Prog. Sci. Transl., Transl. 71].

Leavesley, G. H., R. W. Lichty, B. M. Troutman and L. G. Saindon, (1983), "Precipitation-Runoff Modeling System--Users manual:," Water Resources Investigations Report 83-4238, U.S. Geological Survey.

Male, D. H. and D. M. Gray, (1981), "Snowcover Ablation and Runoff," Chapter 9 in Handbook of Snow, Principles, Processes, Management & Use, Edited by D. M. Gray and D. H. Male, Pergammon Press.

Marks, D. and J. Dozier, (1979), "A Clear-Sky Longwave Radiation Model for Remote Alpine Areas," Archev Fur Meteorologie Geophysik und Bioklimatologie, Ser B, 27: 159-187.

McDonnell, J. J., M. Bonell, M. K. Stewart and A. J. Pearce, (1990), "Deuterium Variations in Storm Rainfall: Implications for Stream Hydrograph Separation," Water Resources Res., 26(3): 455-458.

McDonnell, J. J., M. K. Stewart and I. F. Owens, (1991), "Effects of Catchment-Scale Subsurface Mixing on Stream Episodic Isotopic Response," Water Resour. Res., In press.

Meiman, J. R., I. Friedman and K. Hardcastle, (1974),"Deuterium in Rocky Mountain snowpacks," Snow and Ice Resources, Monterey, California, 152-160.

Mock, N. A., (1988), "A Hydrological Characterization of Zero-Order Basin in Volcanic Hillslope Terrain," MS Thesis, Civil Engineering, Utah State University.

Moore, R. D., (1989), "Tracing Runoff Sources with Deuterium and Oxygen-18 During Spring Melt in a Headwater Catchment, Southern Laurentians," Quebec J. Hydrol., 112: 135-148.

Neale, C. M. U., (1991),"An Airborne Multispectral Video/radiometer System for Agricultural and Environmental Monitoring," Symposium on Automated Agriculture for the 21'st Century, Chicago, December, ASAE, 293-299.

Rodhe, A., (1987), "The Origin of Streamwater Traced by Oxygen-18.," Ph.D. Thesis, Uppsala University, Sweden.

Rosenberg, N. J., (1974), Microclimate The Biological Environment, John Wiley & Sons, Inc., 315 p.

Satterlund, D. R., (1979), "An Improved Equation for Estimation Long Wave Radiation from the Atmosphere," Water Resources Research, 15: 1649-1650.

Sklash, M. G. and R. N. Farvolden, (1979), "The Role of Groundwater in Storm Runoff," Journal of Hydrology, 43: 45-65.

Stephenson, G. R., (1977), "Soil-Geology-Vegetation Inventories for Reynolds Creek Watershed," Miscellaneous Series No. 42, Agricultural Experiment Station, University of Idaho.

Stichler, W., (1987), "Snowcover and Snowmelt Processes Studied by Means of Environmental Isotopes," In Seasonal Snowcovers: Physics, Chemistry, and Hydrology, Edited by In:, 211, D. Reidel, Dordrecht, p.673-726.